# Influence of Wind Turbines on Seismic Records of the Gräfenberg Array

by Klaus Stammler and Lars Ceranna

## ABSTRACT

Continuous seismic signals of wind turbines (WTs) have been analyzed at 13 sites of the Gräfenberg (GRF) array in Germany. The stations of the GRF array have operated continuously for 40 years and comprise the longest available digital broadband array data set. By comparing time spans before and after installation of WTs in the vicinity of the stations, their influence on background noise can be quantified. Here, a strong dependence is shown between local wind speed and the observed effects on noise spectra. Station sites with WTs within distances up to 5 km are exposed to significant disturbance in the background noise; even at distances of 15 km such signals are still visible. The geological setting at GRF with sedimentary layer below all stations seems to favor propagation of these signals. Moreover, we observe different decay patterns for signals below and above 2 Hz, which could be related to the geometry of this layer. Overall, our observations clearly document deteriorating effects of WTs to highly sensitive seismological stations.

## INTRODUCTION

In the years 1975–1980, 13 stations of the Gräfenberg (GRF) array (Harjes and Seidl, 1978) have been installed in the Frankonian mountain range in southern Germany (see Fig. 1). Since that time they are recording continuous digital seismic broadband array data and therefore provide a worldwide unique data set for 40 years. The array has an aperture of ~50 km in east–west direction and 100 km in north–south direction. Aiming on similar recording conditions, the geometry of the array was adapted along areas of comparable shallow geologic structures, in this case a layer of sedimentary rock (karstified limestone). Originally, the array has been designed for the observation of global events. However, in recent years, the monitoring of local seismicity is of increasing importance even in regions with low-tectonic seismicity, mainly driven by monitoring induced seismicity due to mining activities. Furthermore, the data set contains records of nuclear explosions since 1975, which serves as reference ground-truth database for possible future explosions at known test sites. Therefore, this unique data set with its seismological fingerprint is of great importance for the Federal Institute for Geosciences and Natural Resources as National Data Center for the compliance with the Comprehensive Nuclear-Test-Ban Treaty (CTBT) as a national technical mean.

After the devastating Tohoku tsunami earthquake in March 2011 with the coseismic generated breakdown of the Fukushima nuclear power plant, the German government has decided to restructure the energy supply in Germany, which has led to an immense increase in wind turbine (WT) installations. In the recent years, a number of WTs have also been installed in the vicinity of the GRF array stations (see Table 1). Imprints of WTs on seismological records were investigated earlier by Styles *et al.* (2005) and Saccorotti *et al.* (2011). Their studies, based on measurements using temporary instrument installations, find influences of WTs at seismic records beyond 10 km distance at frequencies of 1.7 Hz and above (Saccorotti *et al.*) and 3.5 Hz and above (Styles *et al.*). Styles *et al.* recommend a WT free zone with a radius as large as 17.5 km combined with the concept of a noise budget to protect the British CTBT station Eskdalemuir in Scotland against seismic WT influences. However, the situation at the GRF array with WT installations in different distance ranges close to high-quality permanent seismological stations over decades including long-term recordings before and after WT installations provides a much clearer picture for analyzing in detail the generation of seismic noise signals by wind power plants.

The noise signals are generated by the tower of the WT, excited by the rotating blades. The emitted spectrum is controlled by the eigenfrequencies of the whole construction and their multiples together with the timely varying blade-passing frequency coupling into the ground via the base plate. Irrespective of the coupling into the ground, the radiated energy scales with the wind as the driving force. Therefore, high-WT noise signals are expected at high wind speeds and vice versa—lower signals at low wind speeds.

## DATA PROCESSING

A systematic study of these noise effects is performed by processing continuous vertical-component data at all stations for two years. Hourly noise spectra (power spectral densities [PSDs]) are computed and averaged over times with comparable wind speeds. These wind-dependent, averaged noise spectra are compared for time spans before and after installation of WTs in the area of the GRF array to reveal changes originating from these additional noise sources. The wind speed data (10 m above ground) were taken from the European Centre for Medium-Range Weather Forecasts (ECMWF; see Data

doi: 10.1785/0220160049

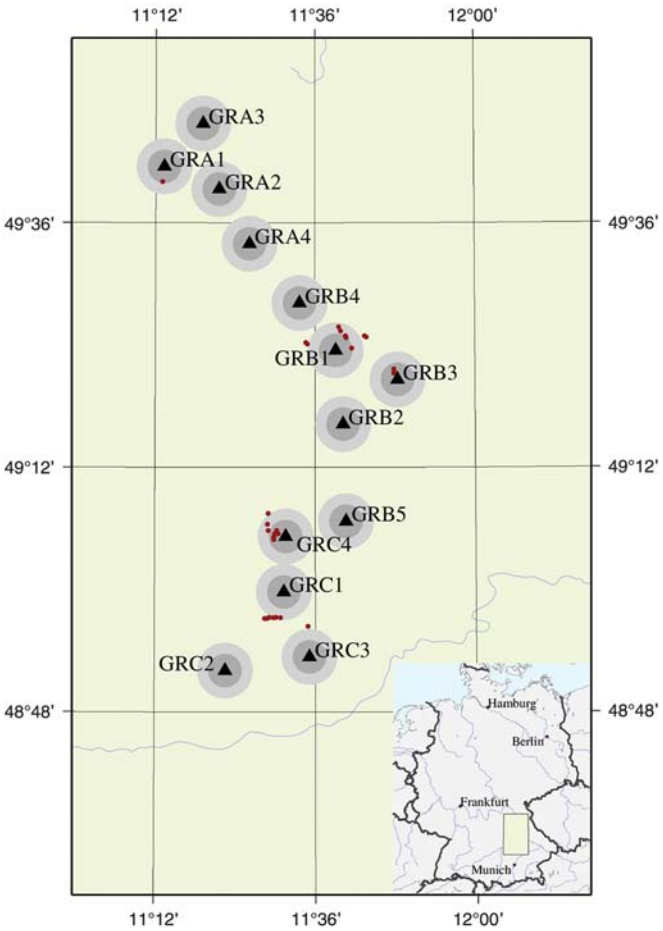


▲ **Figure 1.** The stations of the Gräfenberg (GRF) array (black triangles) in southeastern Germany with an aperture of about 50 km × 100 km. The circles mark ambient areas within 3 km (dark gray) and within 5 km (light gray) radius. Red dots indicate the locations of the closest wind turbines (WTs) within 7 km distance to each station. Note that there are many more WTs (about 200) outside the marked areas. Their exact location is unfortunately not publically available and therefore cannot be reproduced on this map. Map created using Generic Mapping Tool (GMT; see Data and Resources). The small map in the lower right corner indicates the location of array within Germany (green rectangle).

and Resources) data set, providing a resolution in time of 6 hr. Moreover, a single location near the center of the array of the wind data was used for all GRF stations assuming the same wind conditions at all sites. The ECMWF data set is well-suited for this approach because it is free of local wind effects compared with specific wind measurement sites. Local wind speed data were not available at any of the GRF station sites. The processing steps for the seismic data were as follows:

- Split the continuous data of a year into one-hour segments.
- Exclude those traces that contain extremely high-amplitude values compared with noise (above 5000 nm/s), that is, excluding data with recordings of earthquakes.
- Minimize industrial noise from the traces by applying appropriate notch filters (see the Suppression of Industrial Noise Peaks section).
- Compute the PSD spectra of the one-hour segments (Press *et al.*, 1986).
- Bin the obtained spectra by wind speed values (steps of 1 m/s) and averaged (75% quantile) in each interval. The computation of sums instead of quantiles leads to similar results.
- Finally, smooth the averaged spectra moderately (width 0.05 Hz).

## SUPPRESSION OF INDUSTRIAL NOISE PEAKS

From the very beginning, the records of the GRF array contain signatures of industrial noise caused by a number of industrial facilities situated in the area of the GRF array. Closer investigation of such signatures shows that they are of nearly monochromatic character, exist within repeating time windows of a few hours length, and are stable in frequency usually over months. Therefore, these disturbing signals can be removed by a series of sharp notch filters. For each station and each hour of data, a unique filter set is composed and applied. Most notch filters have a width of only 0.01 or 0.02 Hz, a few have widths of 0.03 or 0.04 Hz, and only in rare exceptional cases filter widths of up to 0.2 Hz have to be applied in the frequency band above 4.5 Hz. Applying statistics on the notch filters shows that the sources of these signals are in many cases local to a single station, some noise sources affect several neighbored stations (same peak frequency at the same time), but no such noise peak is visible throughout the whole array. Overall, the data are cleaned from monochromatic machine noise applying these notch filter sets before further data processing. It should be mentioned that the application of these notch filters is not crucial for the identification of the WT noise because it only removes some distracting peaks in some of the spectra and shows that in contrast to the WT signals this monochromatic noise can be easily removed in the frequency domain.

The noise created by WTs is absolutely unaffected by this processing because it differs significantly from such machine noise, as the WT-generated noise disturbs a broad frequency range and not only narrow bands in the spectrum. Furthermore, this WT noise is created at all stations by a common source exciting similar frequencies at the same time (during periods with increased wind speeds) on all stations affected, deteriorating earthquake signals throughout the whole array.

## RESULTS

The obtained spectra are shown in the frequency window between 1 and 7 Hz applying the above procedure. We chose this frequency window because this frequency range is of high relevance for seismic records at GRF, for teleseismic events, as well as for regional and local events. At lower frequencies, the spectra are dominated by the microseismic peaks, and we did not find evidence for a strong influence of the local wind speeds

**Table 1**
**Closest Wind Turbines (WTs) above 1 MW Nominal Power to Each of the Stations of the Gräfenberg Array**

| Name, Number of WTs | Distance Range (km) | Type of WTs |
|---|---|---|
| GRA1 1 | 2.7 | Enercon E-66 |
| GRA2 0 | – | No WT within 10 km |
| GRA3 0 | – | No WT within 10 km |
| GRA4 0 | – | No WT within 15 km |
| GRB1 5 | 3.1–3.8 | Nordex N117, Vestas V112 (plus five WT between 4 and 6 km) |
| GRB2 11 | 7.0–9.0 | Enercon E-82, REpower 3.2 M114 |
| GRB3 3 | 1.4–2.1 | REpower 3.2 M114 |
| GRB4 3 | 7.2–8.4 | Nordex N117, Vestas V112 |
| GRB5 0 | – | No WT within 10 km |
| GRC1 6 | 4.6–5.8 | Enercon E-92 |
| GRC2 3 | 7.4–8.1 | Nordex N117, Enercon E-66 |
| GRC3 1 | 5.7 | Vestas V90 |
| GRC4 5 | 1.4–2.1 | REpower 3.2 M114 (plus three WT between 3 and 6 km) |

The information about the WTs is taken from the Bavarian Energy Atlas (Energie-Atlas Bayern; see Data and Resources) and from approving authorities.

compared with the wind dependence inferred from sources located in the Atlantic Ocean or North Sea. Higher frequencies were not systematically studied as we were using mainly 20 Hz data streams so far. Furthermore, we found indications that at high frequencies the emitted turbine signals decay at rather short distances. The resulting spectra for station GRB3 are shown in Figure 2a,b. In Figure 2a, the noise spectra recorded in the year 2011 is displayed; at that time no WTs existed in the vicinity of this site. The different colors represent the noise spectra at different wind speeds, from almost no wind (blue, 0–2 m/s average wind speed) in steps of 1 m/s up to above 6 m/s (red). The spectral lines are very close to each other indicating that there is no significant wind dependence of the noise level. However, this picture changes completely when looking at data of the year 2014 (Fig. 2b), when three WTs are operated in distances of 1.4, 1.6, and 2.1 km to GRB3. The 2014 data demonstrate that the noise spectra are, in contrast with the 2011 data, strongly dependent on wind speed showing a change of noise level up to two decades. To illustrate the evolvement of the turbine noise signals in time, Figure 3 shows hourly based PSD spectra in a spectrogram-like display for the year 2013 when the WTs started operation. 7682 spectra of this year computed with the same procedures as used in Figure 2 are color coded in amplitude and stacked in chronological order along the vertical axis. All three turbines at GRB3 started operation in August 2013, which has been confirmed by the approving authority of the WTs. From this time onward, the red areas in the upper part of Figure 3 indicate the high amplitudes of the turbine-generated noise. The amplitude variations in time are effects of the varying wind speed. This figure clearly identifies the WTs as the origin of the observed increased wind-dependent noise. A similar situation exists for station GRC4 in which 2011 also no significant wind dependence is visible (Fig. 2c,d). In the year 2014, after installation of five WTs in the distance range between 1.4 and 2.1 km (plus additional ones at 3.3 km and more), the noise level increased at high wind speeds and is of the same order as at GRB3. Here, almost all frequencies between 1 and 7 Hz are affected.

At another site GRB1, five WTs are installed between 2012 and 2013 in a distance range between 3.1 and 3.8 km plus five additional ones between 4.4 and 6.0 km. Overall, the comparison of the spectra from the years 2011 and 2014 in Figure 2e,f shows here that the frequencies between 2 and 7 Hz are less disturbed as compared to stations GRB3 and GRC4 according to the larger distances of the WTs to the seismic station. Interesting, however, is the high-WT generated noise between 1 and 1.5 Hz leading to the highest noise peak (~20, 000 nm/s) measured in this analysis of GRF stations. We notice decaying amplitudes with distance for frequencies above 2 Hz, whereas frequencies close to 1 Hz show a different behavior.

Looking first at the higher frequencies, we notice that all observed WTs emit seismic energy between 3.3 and 4.0 Hz. Therefore, we try to estimate a signal decay law with distance from the WT within this frequency window. We compute the 75% quantiles of all spectra recorded at wind speeds between 5 and 7 m/s and determine the maximum noise peak between 3.3 and 4.0 Hz for each GRF station. To allow a rough estimation of the signal decay, we need to introduce at each station a reference distance for the set of neighboring WT installations. Because closer WTs contribute stronger signals than WTs further away, we chose the harmonic mean of all station-to-WT distances as the reference distance. Assuming a signal summation in amplitudes of $\sqrt{N}$, we divide the PSD value (containing squared amplitudes) by $N$, the number of contributing WTs, to estimate the influence of a single WT at the reference point. The result in Figure 4 shows these estimated single WT signal strengths (vertical axis in $nm^2/s$) versus the distance between station site and WT towers in kilometers (red dots). The orange bars represent the raw data, that is, the measured PSD value at each station. The length of each bar indicates the distance range of the considered WTs, and the width of the bar is proportional to the number of WTs. It can be seen that the (heuristic) introduction of the reference distance as the harmonic mean and the normalizing procedure lead to a consistent decay pattern. Assuming a power-law decay proportional to $1/r^{\beta}$, we get a quite good fit of the decay in PSD values (red dots) in the order of $\beta = 2.7$ if we exclude station GRA1 (white dot in Fig. 4). At GRA1, the WT was installed in January 2000 and therefore is about 15 years older than the modern towers at all other stations and therefore might emit considerably different noise amplitudes explaining the outlier position of this point. The average PSD noise level at the GRF stations in this frequency window (3.3–4.0 Hz) is at ~50 $nm^2/s$ (using 75% quantiles for medium wind speeds between 3 and 4 m/s,

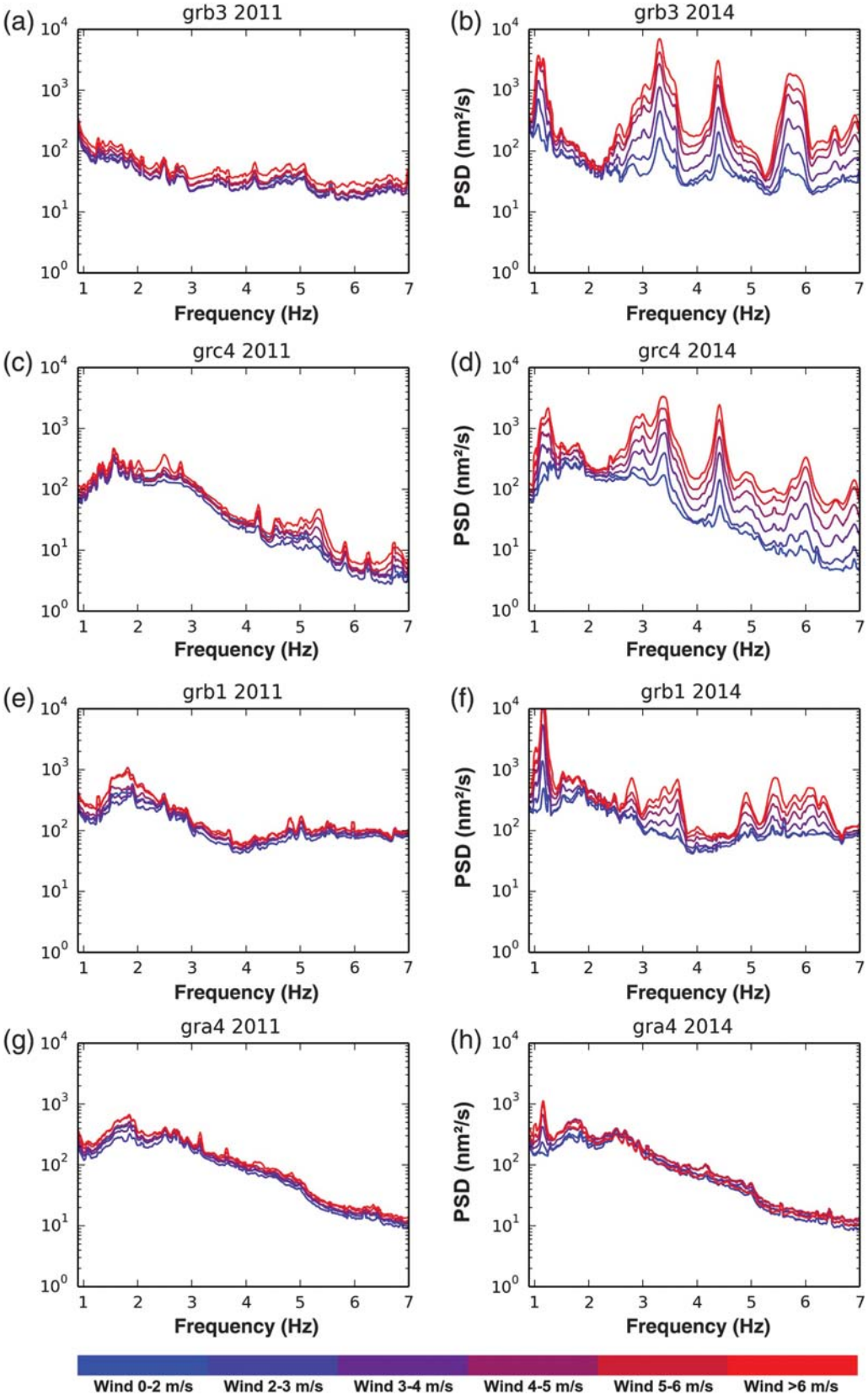


▲ **Figure 2.** Power spectral density (PSD) noise spectra (in $nm^2/s$) between 1 and 7 Hz for the stations GRB3, GRC4, GRB1, and GRA4 of the years 2011 (left) and 2014 (right). The colors of the lines indicate different wind speeds from blue (below 2 m/s) to red (above 6 m/s). Between 2011 and 2014, a number of WTs have been installed at GRB3 (three turbines in 1.4–2.1 km distance range), GRC4 (seven turbines in 1.4–3 km distance range), GRB1 (five WTs in a distance range between 3.1 and 3.8 km), and GRA4 (many turbines in distances larger than 15 km).

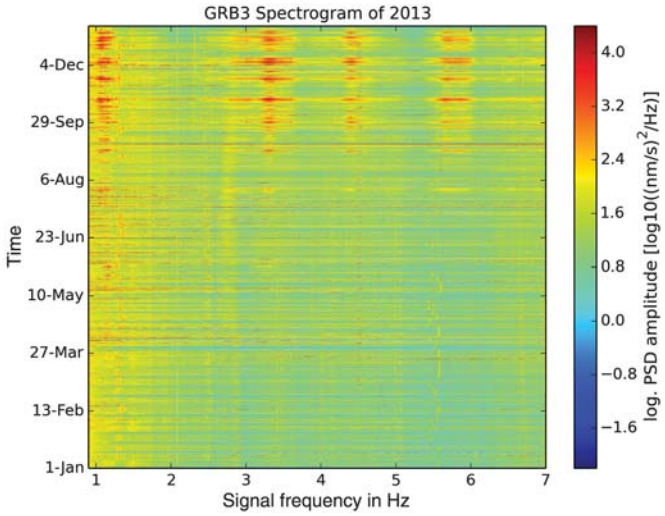


▲ **Figure 3.** Spectrogram-like display of the noise spectra of station GRB3 recorded in the year 2013. PSD spectra of 1 hr segments are color coded in amplitude and stacked along the vertical axis to show the evolvement in time of the turbine noise. The horizontal axis shows the linear frequency range between 1 and 7 Hz (as in Fig. 2). After August 2013, when three WTs started operation clearly increased noise signal can be identified (red areas in the upper part of the figure).

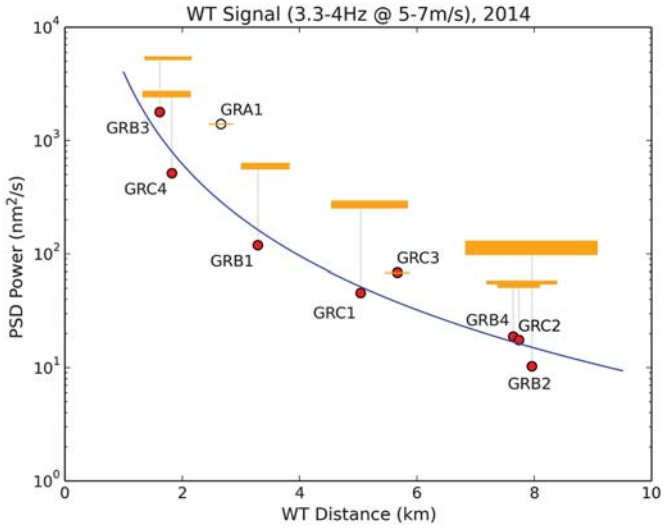


▲ **Figure 4.** WT signals (PSD in $nm^2/s$, vertical axis) between 3.3 and 4.0 Hz at wind speeds between 5 and 7 m/s recorded at different GRF stations and plotted versus the distances of the WTs to the stations. The orange bars show the raw data, that is, the measured PSD value at each station. The length of bar indicates the distance range of the closest stations, and the width of the bar is proportional to the number of WTs in that distance range. The red dots show the reference distance (harmonic mean of the closest stations) and a normalized PSD value (observed value divided by the number of WTs). The vertical gray lines connect the raw data with the corresponding normalized and labeled data point at the reference distance. A fit through the red dots (blue line) yields a power-law decay of −2.7 in PSD values. Station GRA1 (white dot) is disregarded in the fit due to a much older WT than used at the other sites.

summing traces and averaging between 3.3 and 4 Hz). The WT signals decay down to that order at ~5 km distance by applying our curve fit. This means that we do not expect significant WT noise contributions in this frequency range at medium wind speeds from WTs at distances larger than 5 km.

However, the picture changes dramatically when considering frequencies close to 1 Hz: As shown in Figure 2f, the largest peak is not at the sites with WT distances below 2 km but at the site GRB1 with WT distances between 3 and 5 km. Similarly, station GRA4 shows a comparably strong WT noise signal originating from distant sources (> 15 km; see Fig. 2g, h). In fact, the 1.15 Hz signal is visible at all 13 sites of the GRF array with the largest peak near the array center (at GRB1) and decaying amplitudes at array sites to the north and the south, respectively. Therefore, the formulation fails for a power-law decay unlike the previously investigated higher frequencies, as documented in Figure 5. This figure shows a similar plot as in Figure 4, but for the lower frequencies around 1.15 Hz. Here, no consistent decay pattern can be recognized neither in the raw data nor after normalizing to a reference distance. Possible explanations for this behavior at low frequencies would be:

1. a major source at this frequency close to the center of the array decaying in amplitude to the north and south,
2. different spectra emitted by the various types of WTs close to 1 Hz leading to a type-driven distribution of the 1.15 Hz peak heights among sites,
3. resonance effects within the limestone layer with focusing and defocusing of signals, which are mainly driven by the layer thickness rather than distances between stations and WTs.

To further investigate the source of this signal, the time history between 2010 and 2015 of the 1.15 Hz value of the PSD spectrum at six selected stations of GRF array is analyzed. The long-time average (~120 days) of PSD values at the frequency of 1.15 Hz at hours during a mean wind speed of $4.0 \pm 0.2$ m/s are plotted versus time in Figure 6, showing the time history of the 1.15 Hz signal for these GRF stations over five years from mid-2010 to mid-2015. This wind speed window was chosen because we intended to have similar wind conditions for averaging and a value well below the maximum observed speed, which provides a large enough data set for the averaging process. It can be clearly recognized that there is no increase of the noise until 2012. However, with the installation of the first WTs in 2012, all stations synchronously show higher noise signals. Since 2012, the number of WTs in the area has steadily been increased resulting in growing noise signals. Although, there is some variation in the slope of the increment, the overall trend of the noise signal is upward from 2012 to 2015. The only clear and large jump in PSD values is at GRB1 in February 2013, which can be attributed to the installation of seven Nordex N117 and three Vestas V112 turbines. The other stations show a signal increase over years without clear

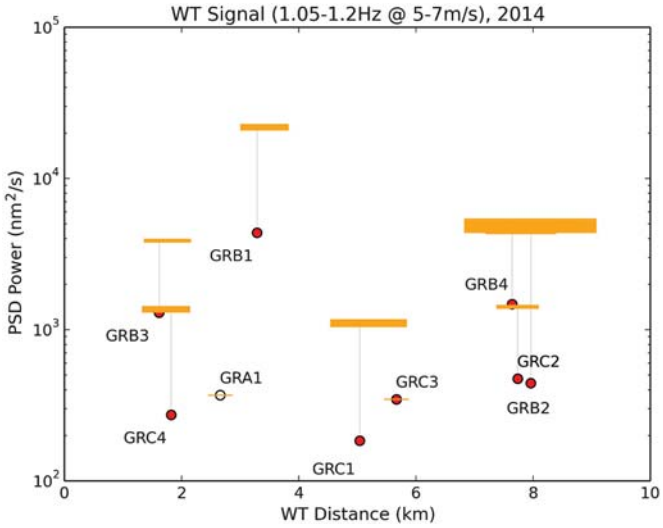


▲ **Figure 5.** Similar graph as in Figure 4, but for lower frequencies between 0.5 and 1.2 Hz. The orange bars show the raw data (PSD values) and the red dots the normalized values at the reference distance (details see Fig. 4). No consistent decay pattern can be recognized for WT signals in this frequency range.

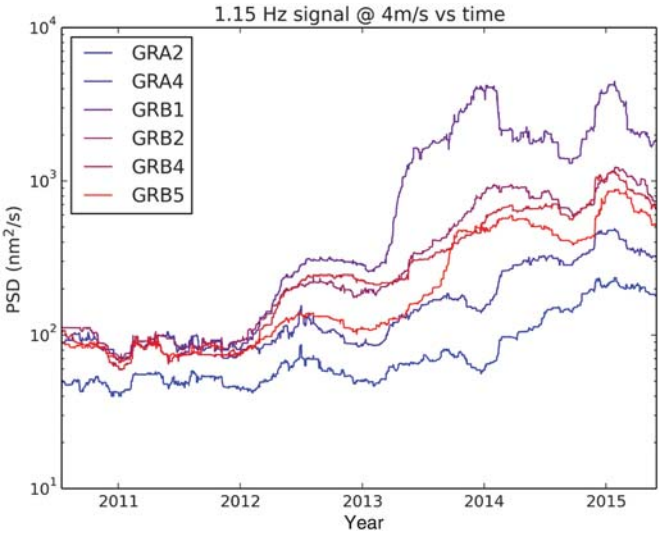


▲ **Figure 6.** Smoothed time history of the WT signal (PSD in $nm^2/s$) at 1.15 Hz at a wind speed of 4.0 ± 0.2 m/s (long-time average, ~120*d*) at six stations of the GRF array. Since 2012, many WTs in the area of the GRF array have been installed resulting in a steady increase of the signal. The jump in the PSD value in February 2013 at station GRB1 is attributed to the installation of seven Nordex N117 and three Vestas V112 turbines within a 6-km distance to GRB1.

identification of installations of specific WTs. This means that the possibility of single strong sources affecting all sites at the same time (explanation 1 from above list) can be ruled out. The observations are, at least, not in contradiction to the explanation (2) of accumulated vibrations in the sediment layer below all GRF stations. Such a resonant stationary wave could be induced by the entirety of WT installations in the whole area. Taking the local geological structure into account, which is described by Krüger (1994), a prominent limestone layer with an average thickness of a few hundred meters can be identified in this area. The bottom of the limestone can be described by the first-order discontinuity yielding a persistent ducting of the WTs' noise energy in this layer. However, the data do not allow to distinguish between explanations (2) and (3). It is probable that both effects partly contribute to the observations, but more investigations are needed to address this in detail.

Finally, we compared recordings at GRA1 with those measured at the collocated borehole instrument GRFO at ~100 m depth below surface. Both spectra are similarly affected by a single WT that is installed in 2.7 km distance (see Fig. 7). This clearly documents that at least signals with frequencies up to

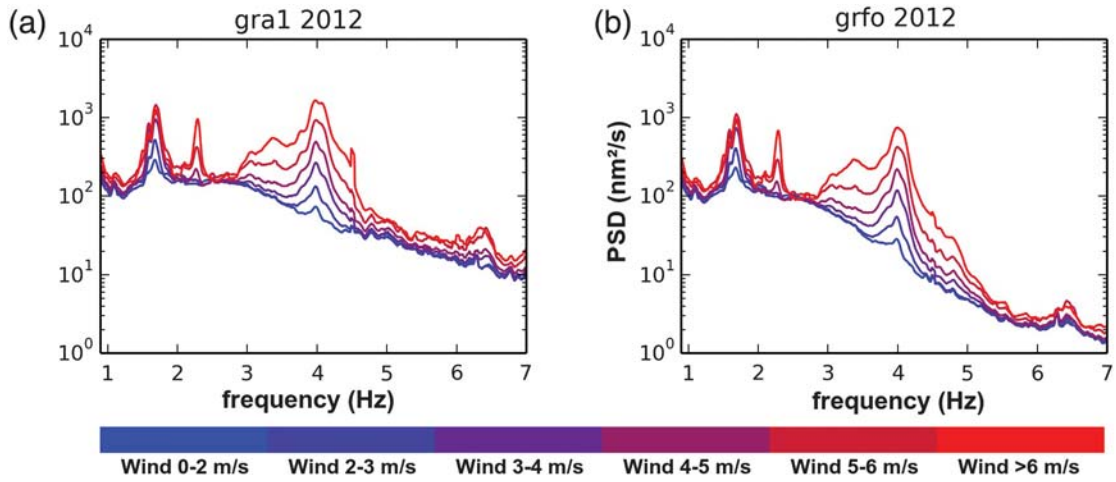


▲ **Figure 7.** PSD noise spectra (in $nm^2/s$) between 1 and 7 Hz for (a) station GRA1 and (b) the collocated borehole station GRFO of the year 2012. The instrument in GRFO has a depth of 100 m below the surface. The colors of the lines indicate different wind speeds from blue (below 2 m/s) to red (above 6 m/s). One WT in the distance of 2.7 km to GRA1 is operated.

~5 Hz penetrate into such depth. This is also consistent with the assumption of a wavelength of ~200 m for a 5-Hz signal at an *S*-wave speed of approximately 1 km/s within the limestone layer and proofs that we are dealing with such wave dimensions and are not confined to near-surface effects at very low propagation speeds.

## SUMMARY AND CONCLUSIONS

WTs introduce a significant wind dependence of the noise spectra of all GRF stations. No such effect could have been observed in the absence of such devices in many years of operational GRF stations. The WT signals reduce the sensitivity of the GRF stations in large parts of the frequency range between 1 and 7 Hz, which are crucial for the analysis of seismic events. Because all stations of the GRF array are affected at ~1 Hz and many stations also above 2 Hz, the sensitivity of the array as a whole has been already significantly degraded at medium and high wind speeds. In particular, installations within a distance range of 5 km lead to significantly deteriorated noise spectra as could be shown at the sites GRB3, GRC4, and GRB1. WTs within this distance lead to increased noise levels at all emitted frequencies in the range studied here (1–7 Hz). This could be shown explicitly for signals between 3 and 4 Hz, which follow an approximate power-law decay of $\beta = 2.7$ and yield to a fade away below the background noise level at distances larger than approximately 5 km. Low frequent WT signals at ~1.15 Hz are visible within a much larger radius (more than 15 km). Therefore, additional installations of WTs in a distance range within at least 5 km should be omitted at all sites of GRF to preserve the still remaining sensitivity and high data quality at the individual sites and on the array beam trace of GRF. However, the long-period WT signals with a center frequency of ~1.15 Hz do not show a consistent decay and spreading pattern, the strength of the signals seems to be dominated either by the emitted spectrum of the closest WTs or by the propagation effects of these low frequent signals within the limestone layer or by a superposition of both effects. Further investigations are needed to provide possible explanations for these observations.

Even though the observations in this study are based on data of the GRF array and are made in a specific geological environment, we think at least parts of the observations are of principal relevance and therefore have to be expected also at other seismic station sites with WTs in their vicinity. The numbers found here for amplitude decay and critical distances may not be valid at other locations, but a critical view on planned WT installations within a few kilometers to highly sensitive seismic stations is advisable.

## DATA AND RESOURCES

The wind speed data used in this study were taken from the European Centre for Medium-Range Weather Forecasts (ECMWF; see http://www.ecmwf.int, last accessed May 2016). Figure 1 was made using the Generic Mapping Tool (GMT) v. 4.5.6 (www.soest.hawaii.edu/gmt, last accessed June 2016; Wessel and Smith, 1998). The locations of the wind turbines are taken from the Energie-Atlas Bayern (Bavarian Energy Atlas, in German) at https://www.energieatlas.bayern.de (last accessed May 2016). All seismic data were taken from our own data center at the Federal Institute for Geosciences and Resources (BGR, see http://www.bgr.bund.de, last accessed May 2016). All data are publically available, for example, via the arclink protocol and International Federation of Digital Seismograph Networks (FDSN) webservices (see http://www.orfeus-eu.org/eida/eida.html, last accessed May 2016).

## ACKNOWLEDGMENTS

We thank two anonymous reviewers and the editor for their helpful comments to improve this article.

## REFERENCES

Harjes, H.-P., and D. Seidl (1978). Digital recording and analysis of broadband seismic data of the Gräfenberg (GRF) array, *J. Geophys.* **44,** 511–523.

Krüger, F. (1994). Sediment structure at GRF from polarization analysis of *P* waves of nuclear explosions, *Bull. Seismol. Soc. Am.* **84,** no. 1, 149–170.

Press, W., B. Flannery, S. Teukolsky, and W. Vetterling (1986). *Numerical Recipes, The Art of Scientific Computing*, Cambridge University Press, Cambridge, United Kingdom, 818 pp., ISBN 0 521 30811 9.

Saccorotti, G., D. Piccinini, L. Cauchie, and I. Fiori (2011). Seismic noise by wind farms: A case study from the VIRGO gravitational wave observatory, *Bull. Seismol. Soc. Am.* **101,** no. 2, 558–578.

Styles, P., R. England, I. G. Stimpson, S. M. Toon, D. Bowers, and M. Hayes (2005). Microseismic and infrasound monitoring of low frequency noise and vibrations from windfarms: Recommendations on the siting of windfarms in the vicinity of Eskdalemuir, Scotland, *Rept. to MOD/FTI/BWEA*, 125 pp.

Wessel, P., and W. H. F. Smith (1998). New improved version of generic mapping tools released, *Eos Trans. AGU* **79,** no. 47, 579–579, doi: 10.1029/98EO00426.

*Klaus Stammler*
*Lars Ceranna*
*Federal Institute for Geosciences and Natural Resources (BGR)*
*Stilleweg 2*
*30655 Hannover, Germany*
*klaus.stammler@bgr.de*
*lars.ceranna@bgr.de*

Published Online 13 July 2016